Astron. Astrophys. 357, 1115–1122 (2000)

ASTRONOMY AND ASTROPHYSICS

Dynamical behavior of meteoroids in the atmosphere derived from very precise photographic records

Z. Ceplecha, J. Borovička, and P. Spurný

Astronomical Institute of the Academy of Sciences, 25165 Ondřejov Observatory, Czech Republic (ceplecha@asu.cas.cz)

Received 18 January 2000 / Accepted 20 March 2000

Abstract. Basic equations of motion and ablation of a single non-fragmenting body through the atmosphere were solved with ablation and shape-density coefficients as general functions of time. This solution was applied to 22 photographically recorded meteoroids with very precise data available, such meteoroids which did not yield solutions by using the gross-fragmentation model. Extremely high values of the shape density coefficient, K, at the early parts of the luminous trajectory are the main reason for non-existing gross-fragmentation solutions. Reasons for such high values of K are examined in some detail, including analysis of spectral records available for one of the meteoroids. Also positive values of acceleration well outside standard deviations were documented for several meteors. Such cases cannot be interpreted by our model. We suspect that electric forces originating from the atmospheric charges and from meteoroid charges (which were not included in the drag equation) are responsible for the observed very high values of the shape-density coefficient at the early parts of meteoroid trajectories.

Key words: meteors, meteoroids

1. Introduction

In our paper on meteoroid atmospheric fragmentation (Ceplecha et al. 1993), we recognized that most of the photographically recorded meteoroids (double- or multi-station records) behaved according to the single body theory with constant ablation and shape-density coefficients throughout the entire trajectory. About 40% of the studied cases with precision better than ± 30 m for one measured distance along the meteor trajectory exhibited no fragmentation (NF), another 40% exhibited one gross-fragmentation at one point (1F), and about 20% fragmented consecutively at more than one point (MF). The formalistic gross-fragmentation solution for these MF cases was found to be "unrealistic", i.e. the solution usually called for adding mass to the main body at a point instead of releasing part of mass as fragments. We were aware that some of the MF cases with "unrealistic" solutions may not be only due to more fragmentation points, but rather reflect some changes of the ablation and shape-density coefficients (σ and K). In order to study these two coefficients as function of time, we need to use very precise records with distances along the trajectory (and heights) derived with precision of about ± 10 m. We also noted that going to few observations with higher precision, we were not able to apply the gross-fragmentation model at all: both the realistic and the "unrealistic" solutions yielded systematic time dependence of residuals.

In this paper we will derive a complete general solution of the single body theory with ablation coefficient, σ, and shape-density coefficient, K, both as function of time. We will then apply this solution to the most precise photographic observations of meteor trajectories available, in order to derive time change of ablation and shape-density coefficients. We were able to find 22 photographic meteors with such high precision of their records. In all 22 cases we were able to find numerical solutions with precision corresponding to the high precision of geometrically derived data. The smallest standard deviation for one measured point among these 22 cases was found ± 4 m; there are 7 cases with standard deviation of ± 10 m or lower; majority of standard deviations of the used meteors is between ± 10 m and ± 15 m.

2. Basic equations

The motion and ablation of a single non-fragmenting body through the atmosphere can be given by three differential equations (linear trajectory; gravity neglected; curved Earth's surface approximated by an osculating sphere, Ceplecha et al. 1993):

$$\frac{\mathrm{d}v}{\mathrm{d}t} = -\Gamma A \varrho_d^{-2/3} \varrho m^{-1/3} v^2 \tag{1}$$

$$\frac{\mathrm{d}m}{\mathrm{d}t} = -\frac{\Lambda A}{2\xi} \varrho_d^{-2/3} \varrho m^{2/3} v^3 \tag{2}$$

$$\frac{\mathrm{d}h}{\mathrm{d}t} = \frac{l - A/2}{B/2 + h} v \tag{3}$$

$$\frac{A/2 - l}{B/2 + h} = \cos z(t) \tag{4}$$

$$Al + Bh + C = l^2 - h^2 \tag{5}$$

Send offprint requests to: Z. Ceplecha

Two independent parameters of the problem can be expressed as

$$\text{the ablation coefficient} \quad \sigma = \frac{\Lambda}{2\xi\Gamma} \tag{6}$$

$$\text{the shape-density coefficient} \quad K = \Gamma A \varrho_d^{-2/3} \tag{7}$$

For a meteoroid at an arbitrary point of its trajectory, the notation has the following meaning: $v \equiv$ velocity; $t \equiv$ time (independent variable); $m \equiv$ mass; $h \equiv$ height; $l \equiv$ distance along the trajectory; $\varrho \equiv$ air density; $z \equiv$ zenith distance of the radiant (slope to vertical); $\Gamma \equiv$ drag coefficient; $\Lambda \equiv$ heat transfer coefficient; $A = Sm^{-2/3}\varrho_d^{2/3}$ is the shape factor; $S \equiv$ head cross-section; $\varrho_d \equiv$ bulk density of meteoroid; $\xi \equiv$ energy necessary for ablation of a unit mass; A, B, C are constants of the geometrical position of the trajectory.

3. Solutions of the basic equations with constant σ and K

These solutions for $\sigma = \text{constant}$, $K = \text{constant}$ can be found in Pecina & Ceplecha (1983, 1984). They contain 4 parameters of unknown values to be determined from observations: v_∞, σ, v_0, l_0, i.e. initial velocity, ablation coefficient, velocity at $t = 0$, distance along the trajectory at $t = 0$, respectively. We can transform the problem of computing them from the observed distances along the trajectory as function of time into the following linear equation for small increments of these unknowns parameters

$$l_{\rm obs} - l = \frac{\partial l}{\partial l_0}\Delta l_0 + \frac{\partial l}{\partial v_0}\Delta v_0 + \frac{\partial l}{\partial v_\infty}\Delta v_\infty + \frac{\partial l}{\partial \sigma}\Delta\sigma \tag{8}$$

The partial derivatives in (8) can be written as closed expressions and can be found in Pecina & Ceplecha (1983, 1984).

The solution for one gross-fragmentation point, i.e. with $K = \text{constant}$, $\sigma = \text{constant}_1$ before fragmentation, $\sigma = \text{constant}_2$ after fragmentation, was published by Ceplecha et al. (1993), and contains 6 parameters of unknown values to be determined from observations, i.e. $v_{\infty 1}$, $v_{\infty 2}$, σ_1, σ_2, v_0, l_0. In addition two more parameters emerge during the computational procedure, i.e. the position of the fragmentation point on the trajectory, and the relative amount of the fragmented mass, making the total number of parameters to be determined equal to 8. We can once more again convert the problem of computing these parameters into linear equation for their small increments (equations defining the partial derivatives: see Ceplecha et al. 1993) as follows:

$$\begin{aligned} l_{\rm obs} - l \;=\; & \frac{\partial l}{\partial l_0}\Delta l_0 + \frac{\partial l}{\partial v_0}\Delta v_0 + \frac{\partial l}{\partial v_{\infty 1}}\Delta v_{\infty 1} + \\ & + \frac{\partial l}{\partial \sigma_1}\Delta\sigma_1 + \frac{\partial l}{\partial v_{\infty 2}}\Delta v_{\infty 2} + \frac{\partial l}{\partial \sigma_2}\Delta\sigma_2 \end{aligned} \tag{9}$$

$\Delta v_{\infty 1}, \Delta\sigma_1$	$\Delta l_0, \Delta v_0$	$\Delta v_{\infty 2}, \Delta\sigma_2$
before fragmentation	at fragment.	after fragment.

More about these two solutions and about their application to observations can be found also in Ceplecha et al. (1998).

4. General solution of the basic equations with $\sigma = \sigma(t)$, $K = K(t)$

Eliminating mass between Eqs. (1) and (2) we arrive at

$$\log\frac{K}{K_0} = \frac{1}{3}\int_{v_0}^{v}\sigma\, v\,{\rm d}v - \log\frac{\varrho {\rm v}^2}{(-\frac{{\rm d}v}{{\rm d}t})} + \log\frac{\varrho_0 {\rm v}_0^2}{(-\frac{{\rm d}v}{{\rm d}t})_0}, \tag{10}$$

where
$\frac{1}{3}\int_{v_0}^{v}\sigma\, v\,{\rm d}v$ is the ablation term and
$\log\frac{\varrho v^2}{(-\frac{{\rm d}v}{{\rm d}t})} - \log\frac{\varrho_0 v_0^2}{(-\frac{{\rm d}v}{{\rm d}t})_0}$ is the deceleration term.
Here log means natural logarithm. If the ablation term is identically (for all time instants) equal to the deceleration term, then K = constant.

Eq. (10) and $t - t_0 = \int_{l_0}^{l}\frac{{\rm d}l}{v}$ represent a complete solution. Similar numerical procedure as for the case with constant σ and K can be applied to fit the computed distances along the trajectory to the observed distances, except that the partial derivatives cannot be written in a close form and have to be computed by numerical procedures only.

Eq. (10) contains two unknown functions $\sigma = \sigma(t)$, $K = K(t)$. Assuming one of them, the other is resulting from (10). If we could determine $v = v(t)$ as well as $\frac{{\rm d}v}{{\rm d}t} = \frac{{\rm d}v}{{\rm d}t}(t)$ from the observed distances, we would be able to compute $\sigma = \sigma(t)$ and then from Eq. (10) also $K = K(t)$. This will be described in details in the next section.

Once we have solved Eq. (10), mass and ablation are given as

$$m = \frac{K^3\,\varrho^3\,v^6}{(-\frac{{\rm d}v}{{\rm d}t})^3} \tag{11}$$

and

$$\frac{{\rm d}m}{{\rm d}t} = \sigma\, m\, v\,\frac{{\rm d}v}{{\rm d}t} \tag{12}$$

5. Numerical procedures and their testing

In order to find out the most suitable procedure for numerical handling of Eq. (10), we computed several "theoretical meteors". By this term "theoretical meteor" we denote a case, when we have chosen σ and K as a-priori-known functions of time, and then solving Eqs. (1) to (7) by Runge-Kutta method, we derived the "observed" distances along trajectory and "observed" heights as function of time. To such "observed" values, we applied then computational procedures intended to be used for application of Eq. (10) to observations. We have examined several such cases (originating from different combinations of increasing and decreasing σ with increasing and decreasing K). This allowed us to find out the best procedures for application to really observed meteors, and also to formulate several general rules in junction with these solutions.

Our initial idea was to compute parameters for one function of time (given by one formula) applied to all points of the observed trajectory, i.e. to the observed distances along trajectory, l_o, and to the observed heights, h_o. But such procedures (e.g. using interpolation polynomials) proved to be very much

dependent on the chosen function. This was already found by Pecina & Ceplecha (1983) for constant σ and K, and we only generalized this for σ and K being variable with time. We also learned that σ cannot be computed for the early parts of a trajectory, where velocities and decelerations are almost independent of σ. Even a precision of ± 0.1 m used for theoretical meteors did not allow to determine σ during the first third of the trajectory (for range of meteoroid masses we were interested in). This defines our first limitation in applying Eq. (10) even to very precise observational data: for the early parts of a trajectory we must chose only an average value of σ corresponding to the meteoroid type. This limitation has not much influence on K during the early parts of the trajectory, because σ and K are there almost independent. K at the early parts of the trajectory is mostly given by velocity and deceleration, and these can be derived from observed distances along trajectory as function of time.

If we would know v and $\frac{\mathrm{d}v}{\mathrm{d}t}$ from observations, σ could be computed from them, and then also K can be computed from Eq. (10) so as to fit the computed distances along the trajectory, l_c, to the observed distances, l_o. We should be aware that the primary measured values on the photographic records of a meteor, are distances along the trajectory, l_o, and thus fitting them to the computed values by the least squares solves our problem completely. As the best procedure we were able to find, proved to be fitting l_o to l_c for small parts of the trajectory, as small as possible from the point of view of precision. Description of this procedure follows.

We have n consecutive points with known time, t_i, and, at them, we have the observed distances along the trajectory, $l_{o,i}$, and heights, $h_{o,i}$, where $i = 1, 2, ..., n$. We will chose consecutive subsets of m consecutive values from $i = 1$ to m, from $i = 2$ to $(m+1)$, and so on until from $i = (n-m+1)$ to n. We will fit $l_{o,i}$ to $l_{c,i}$ for each of these subsets by the least squares using a polynomial function

$$l_{c,i} = q_1 + q_2 t_i + q_3 t_i^2 + q_4 t_i^3 + q_5 t_i^4 \ , \qquad (13)$$

where q_1 to q_5 are constants to be determined from the respective subset of $l_{o,i}$ values so that sum of $(l_{o,i} - l_{c,i})^2$ is at its minimum value.

Using Eq. (13) is equivalent to using a quadratic expression for approximating deceleration inside the short time intervals of each of the chosen subsets. We will assume that this is strictly valid only for the average time of each of the subsets: thus only q_1, q_2, and q_3 are important for the computed distances along trajectory, and computed velocities and decelerations; the rest is important for computing standard deviations of these values. Thus for each of the above subsets, i.e for average time, t_k, of each subset, we have v_k and $(\frac{\mathrm{d}v}{\mathrm{d}t})_k$ ($k = 1, 2, ..., (n - m + 1)$) from Eq. (13) including their standard deviations. Because generally the average times t_k of the subsets need not to coincide with the actually observed times t_i at which we have available $l_{o,i}$, we can integrate velocities v_k using the original t_i values and determine one integration constant for the entire trajectory in order to fit these computed distances $l_{o,i}$ to the observed distances $l_{c,i}$ for the whole trajectory.

Now, the initial values of σ can be computed from any two neighboring or nearby points on assumption that σ and K are constant on a short time difference. If suffix for the first point is 1, and suffix for the second point 2, then σ is given by ($\log$ is natural logarithm)

$$\sigma = \frac{6[\log(-K_1 v_1^2 \rho_1 (\frac{\mathrm{d}v}{\mathrm{d}t})_2 - \log(-K_2 v_2^2 \rho_2 (\frac{\mathrm{d}v}{\mathrm{d}t})_1]}{v_1^2 - v_2^2} \ , \qquad (14)$$

where t, v, and $\frac{\mathrm{d}v}{\mathrm{d}t}$ are actually the t_k, v_k and $(\frac{\mathrm{d}v}{\mathrm{d}t})_k$, i.e. the average values of each subset. For the start we can chose $K_1 = K_2$, while at the second step, when we already computed values of K from Eq. (10), we can use K_1 and K_2 as different values. We can improve this procedure by taking into account all possible pairs providing that t_1 and t_2 are separated by small time interval, and chose then the best determined values of σ and K (with the relatively smallest standard deviations). We finish with σ and K which best fit the observed distances along the trajectory and correspond to Eq. (10).

In solving Eq. (10) we also need to know K_0, i.e. the value of K at a point, where we start the integration (values of K are only relative in this sense). In our computations we used statistical average of K for the corresponding meteoroid type as K_0, and we have chosen the point at which $K = K_0$ so that σ at this point is also the statistical average for the corresponding type (types I, II, IIIA and IIIB). Numerical values of these constants are in the next section.

6. Application of our model to precise photographic data on individual meteoroids

It is not easy to find out observational data with enough precision for application of Eq. (10) using the procedure described in the preceding section. We inspected several photographic archives of double- and multi-station meteor photographs with the aim not only to find out precise records (with geometrical precision of the trajectory better than ± 20 m), but also records which yielded either no solution for the gross-fragmentation model (or single-body model), or a solution with significant time dependence of residuals, or an "unrealistic" solution. From inspecting over 1000 events by using the gross-fragmentation model (mainly in European and the U.S. archives; McCrosky et al. 1976, 1977; Ceplecha & McCrosky 1997; Spurný 1997), we were able to find out 22 such cases. The results on them are summarized in Table 2. Meaning of individual symbols in Table 2 are as follows: ε_0 is the standard deviation for one measured point as derived by application of the gross-fragmentation model (constant σ and K): residuals show large systematic changes with time for all meteors in Table 2. ε is the standard deviation for one observed point according to solutions presented in this paper, i.e. with σ and K as functions of time: these residuals are almost random with time for all meteors in Table 2. v_B, v_E, and m_B are velocity at the first point, velocity at the last point, and mass at the first point, respectively. Trajectory parts are denoted: B the beginning-, C the central-, and E the end-part. H stands for relatively "high" value, L stands for relatively "low" value, and V stands for "very". "dec-abl" contains the difference between

Table 1. Average values of σ and K for different meteoroid types (groups) on assumption of $\Gamma A = 1.1$

type	ϱ_d g cm^{-3}	σ s^2 km^{-2}	K c.g.s.
I	3.7	0.014	0.46
II	2.0	0.042	0.69
IIIA	0.75	0.10	1.33
IIIB	0.27	0.21	2.63

the deceleration term and the ablation term (it reflects the difference of our present solution against solution with constant σ and K. Symbol "–" means that deceleration term is less than the ablation term, symbol "+" means that the deceleration term is greater than the ablation term, and symbol "=" means that both terms are about equal.

In all computations we used CIRA 72 (1972) model of atmospheric densities using them according to the months in which the meteor was recorded. We found also several cases with precise data, which clearly exhibit large positive (and oscillating) values of $\frac{\mathrm{d}v}{\mathrm{d}t}$, and cannot be explained in scope of Eqs. (1) to (7) (Fig. 10).

Because σ cannot be computed for the beginning parts of a trajectory from observations at all, at such points we assumed average σ value corresponding to the meteoroid type. As standard deviation of so-defined σ value we took 50% of its value (corresponding to statistical uncertainties of the group definitions). Such average values of σ were also used at extreme end of a trajectory in case they were not available from observations (the precision of v and $\frac{\mathrm{d}v}{\mathrm{d}t}$ is also low at extreme end of a trajectory and may not be sufficient for determination of σ). We defined K_0 as corresponding to the meteoroid type, and we started integration of Eq. (10) at a point, where σ corresponded also to the meteoroid type. The numerical values used are in Table 1.

Publishing detailed results would need about 10 plots of different values as function of time for each case. Thus we decided to put all these plots on the Web (Ceplecha et al. 2000). As an example of our results we present data on meteoroid O 27471 in Figs. 1 to 9. In Fig. 10 we present $\frac{\mathrm{d}v}{\mathrm{d}t}$ for one of the cases we found with positive and oscillating values of acceleration. There is not possible any interpretation of these $\frac{\mathrm{d}v}{\mathrm{d}t}$ in the scope of our basic equations.

7. Results

7.1. σ and K as function of time

Table 2 reveals the main reason, why these 22 meteoroids with precise data derived from photographic records did not yield gross-fragmentation solutions with constant σ and K, and with residuals independent of time. In 20 cases from these 22, K is enormously large during the initial part of the trajectory. The gross-fragmentation model assumes K constant, and makes thus the residuals time dependent. We can generalize: if the gross-fragmentation solution proves to be time dependent, we may be

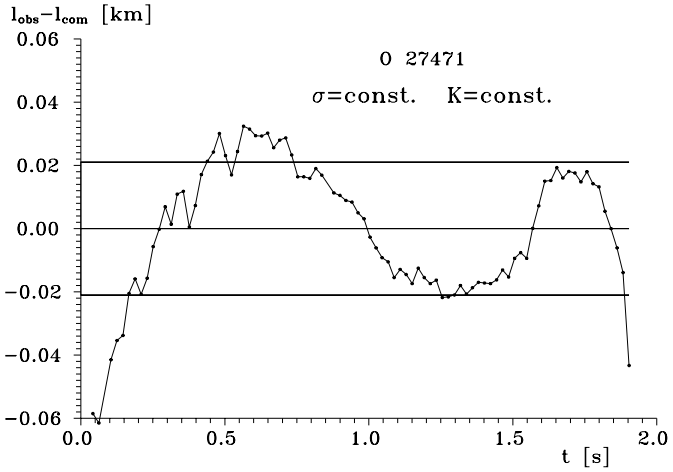

Fig. 1. Residuals for model with constant σ and K. Strong time dependence of residuals is evident. Horizontal lines are the average 0 ± 21 m (the standard deviation for one observed value).

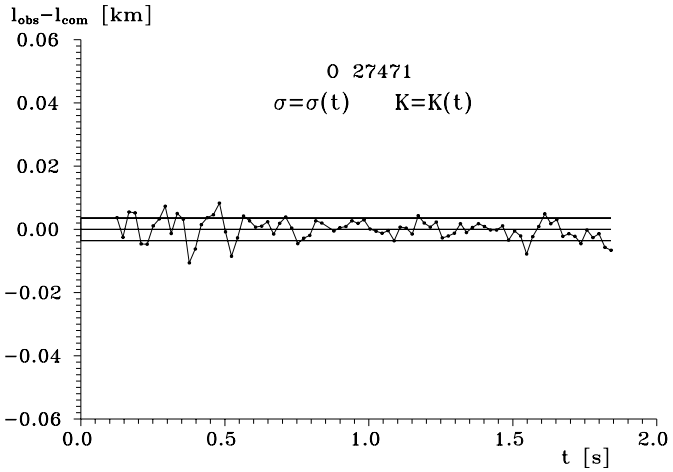

Fig. 2. Residuals for model with σ and K as function of time. Residuals are random with time. Standard deviation for one observed value is ± 4 m.

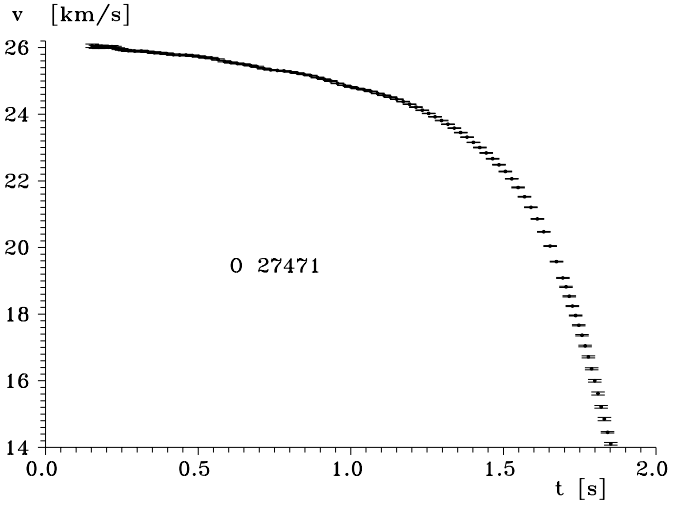

Fig. 3. Velocity as function of time. Standard deviation for each value is given.

Table 2. Survey of results on photographic meteors with precise data.

meteor no.	date	time UT	type	ε_0	ε	v_B	v_E	m_B	σ		K			dec–abl		
	yymmdd	hhmmss		m	m	km s^{-1}	km s^{-1}	kg	C	E	B	C	E	B	C	E
O 24421	60 03 24	21 50 02	II	±5	±4	18.2	13.8	0.43	VH	L	H	L	L	–	–	=
O 27471	60 10 27	00 13 04	I/II	±21	±4	26.1	14.1	1.7	H	L	VH	L	L	–	=	=
O 32202	61 11 02	20 26 36	II	±16	±10	31.4	27.6	2.4	H	L	H	L	L	–	=	+
PN 38737	64 12 07	04 52 12	II	±24	±16	17.2	10.6	180	L	VH	H	L	L	–	+	=
PN 38768	65 01 08	05 01 32	II	±23	±13	17.6	11.6	60	L	H	H	L	L	–	+	+
PN 38827	65 03 08	10 49 39	I	±45	±15	29.3	19.5	0.18	H	L	H	L	L	–	=	=
PN 39122	65 12 28	03 18 48	II	±19	±7	22.5	9.6	80	L	H	VH	H	L	–	=	+
PN 39154	66 01 29	03 53 40	II	±19	±13	21.0	19.5	86	L	H	VH	H	L	–	–	=
PN 39197	66 03 13	07 31 52	I	±14	±4	28.6	25.3	0.02	L	H	L	H	L	=	–	=
PN 39424B	66 10 26	11 10 57	II	±17	±12	26.7	23.2	3.0	H	L	VH	L	L	–	–	=
PN 39476	66 12 17	04 05 28	I	±23	±15	19.6	10.9	0.94	H	L	H	L	L	–	=	=
PN 39499	67 01 09	07 54 18	I	±94	±14	12.4	7.5	80	L	H	H	L	VL	–	=	+
PN 39509C	67 01 19	09 42 24	IIIA	±12	±11	15.5	12.6	14	L	VH	VH	H	L	–	=	+
PN 39608	67 04 28	06 32 54	II	±24	±14	19.6	15.6	6	H	L	H	L	L	–	=	+
PN 39820B	67 11 26	02 04 57	II	±41	±11	16.7	9.4	16	H	H	H	L	L	–	=	+
PN 39828	67 12 04	01 23 05	II	±39	±12	13.6	9.2	6.4	L	H	H	L	L	–	=	+
PN 39938B	68 03 23	06 00 30	II	±16	±13	11.9	8.9	0.84	L	L	H	L	L	–	=	=
PN 40379A	69 06 07	08 10 22	I	±14	±12	16.9	8.9	0.74	L	H	H	L	L	–	=	=
PN 41280	71 11 25	05 49 40	II	±17	±10	13.3	5.8	500	H	L	H	L	L	–	=	=
PN 41432	72 04 25	10 34 41	II	±16	±8	12.7	7.9	160	VH	L	H	H	L	–	–	=
PN 41593	72 10 03	09 25 32	II	±57	±18	22.2	12.6	280	H	VH	L	H	L	–	–	=
PN 41827	73 05 25	03 17 41	II	±27	±8	14.1	8.3	3.1	L	H	H	H	L	–	–	=

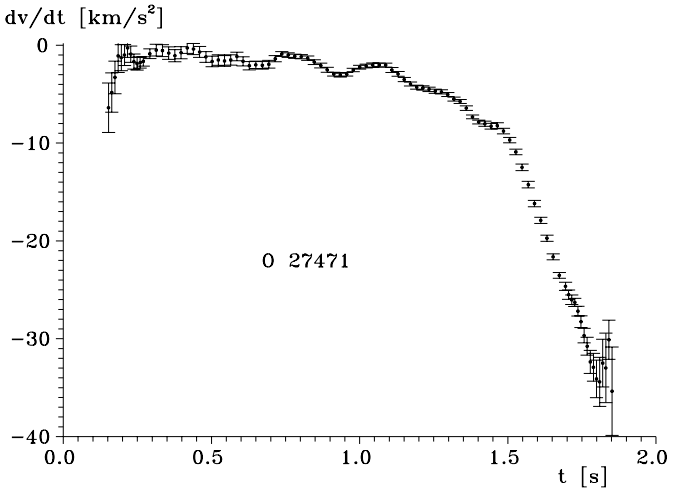

Fig. 4. Deceleration as function of time. Standard deviation for each value is given.

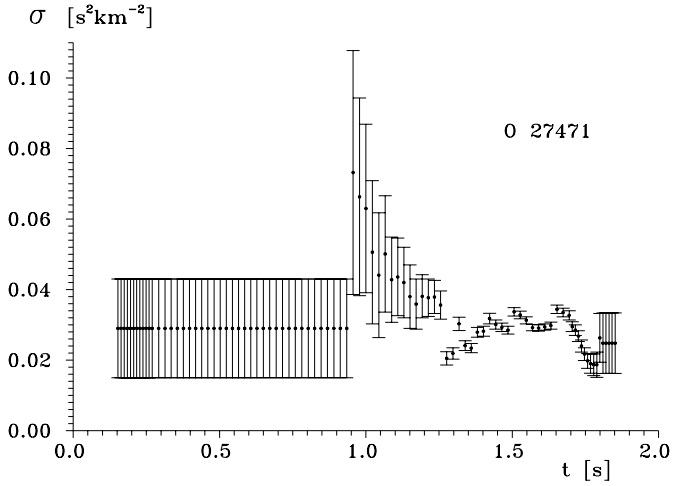

Fig. 5. Ablation coefficient as function of time. Standard deviation for each value is given.

almost sure that the reason lies in very large values of K at the trajectory beginning. The highest value of K we found 54±20 for PN 39122, 42±24 for PN 39154, 19±7 for O 27471, and 16±8 for PN 39424B.

On the other hand σ behaves differently. About half of the cases possess high values of σ at center of the trajectory and half of the cases at the trajectory end. In this sense we can use change of σ as an additional criterion for meteoroid classification into types (I, II, IIIA, IIIB), dividing these types into cases with high continuous fragmentation at the center of the trajectory, and into cases with high continuous fragmentation at the terminal parts of the trajectory. It is well to note that the 2 exceptional cases, when K at the beginning is not high, exhibit the high continuous fragmentation at the terminal part (high σ value at the end of trajectory). In these 2 exceptional cases this seems to be the main reason for not obtaining the gross-fragmentation solutions with time independent residuals.

7.2. Spectral clues

A high resolution spectrum of the bolide O 27471 has been photographed. The spectrum was described by Ceplecha & Padevět

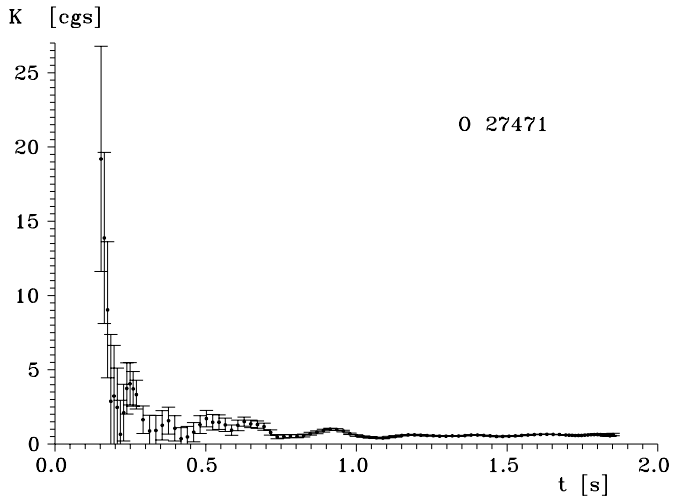

Fig. 6. Shape-density coefficient K as function of time. Standard deviation for each value is given.

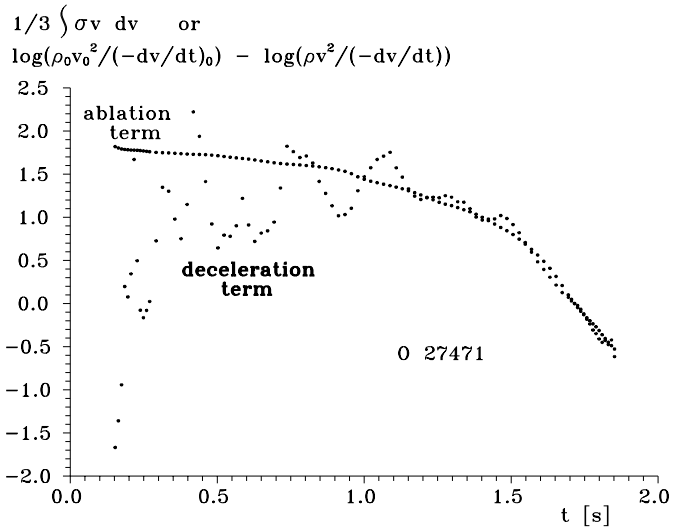

Fig. 7. Comparison of ablation and deceleration terms.

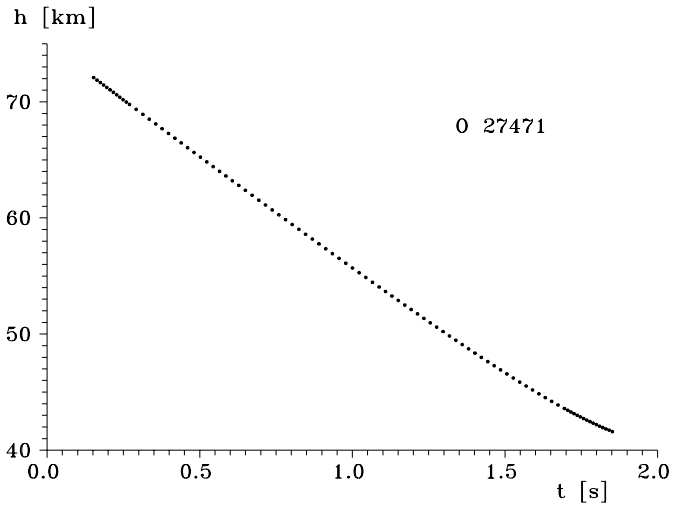

Fig. 8. Height as function of time.

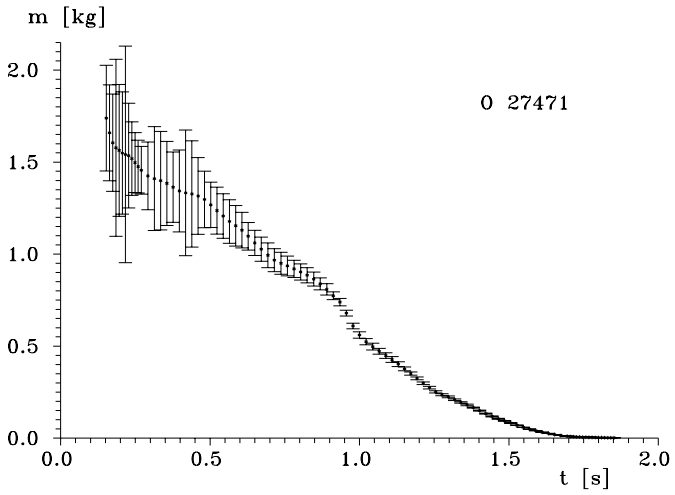

Fig. 9. Mass as function of time. Standard deviation for each value is given.

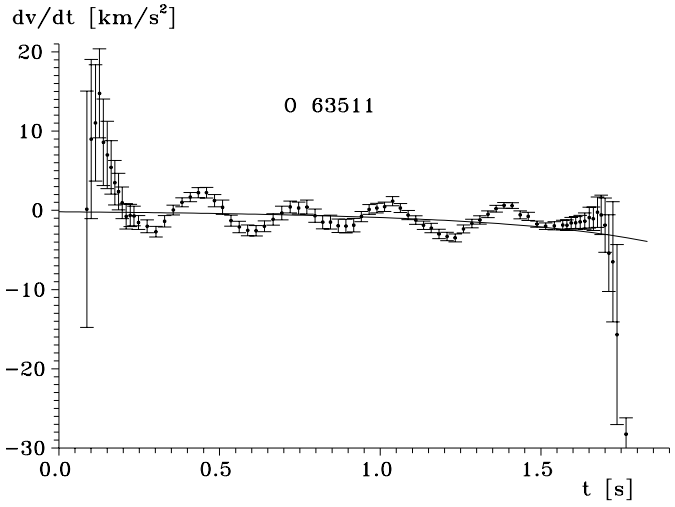

Fig. 10. Acceleration for meteor O 63511 shows regular oscillations outside standard deviations, and into positive values. The smooth line corresponds to solution with σ and K constant. This solution is far from reality. Eq. (1) and procedures of this paper cannot be used for explaining the atmospheric interaction of this meteor.

(1969). For the purpose of this paper we re-measured and re-analyzed the spectrum by the new method of Borovička (1993). The spectrum covers the heights from 84 to 55 km, corresponding to the time from -0.43 to 1.03 s. However, the only visible line at the beginning is the sodium doublet at 5890 and 5896 Å. We were able to analyze the spectrum in detail only between 0.37 and 1.03 s, after the meteor brightened enough to show a sufficient number of spectral lines on the photographic plate. In this interval, K varied nearly by a factor of three, between 0.5 to 1.5 (see Fig. 6).

The spectrum shows no obvious anomalies and no dramatic changes. The lines of Na I, Mg I, Si I, Ca I, Ca II, Cr I, Mn I and Fe I are present. The excitation temperature of the radiating gas was found to be 4800 $\pm$ 200 K along the studied part of the trajectory. The line of Si I is rather strong in this spectrum in

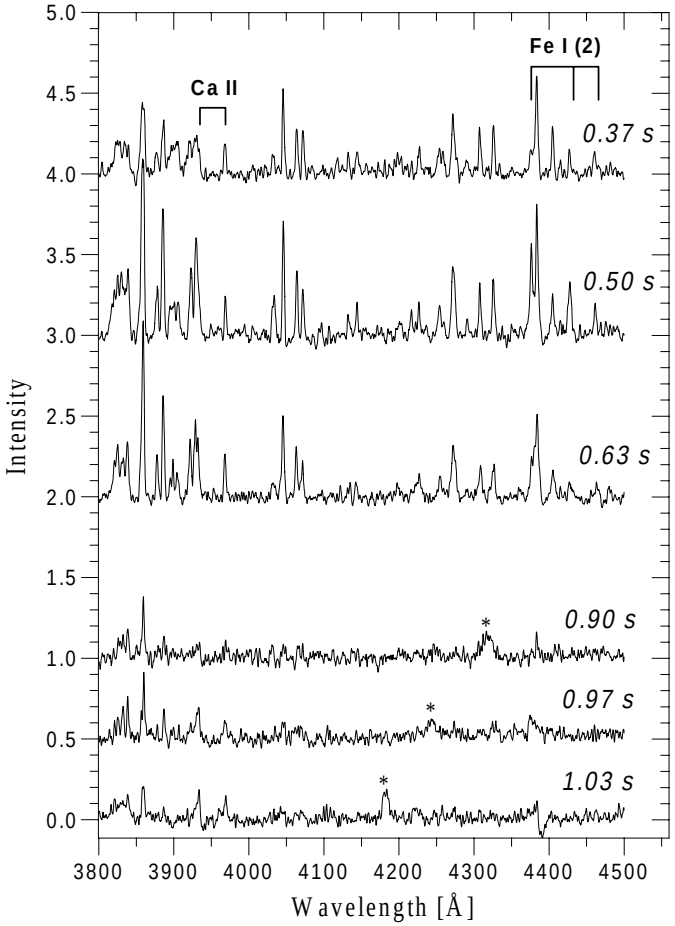

Fig. 11. Blue part of the spectrum of meteor O 27471 at different times. Individual spectra have been shifted vertically for clarity. The lines mentioned in the text are identified. The features marked by asterisk are due to an interfering star trail.

comparison to the spectra of other meteors. Also Mg I is relatively strong, while Na I is somewhat weaker than in other spectra, though still the brightest line in this spectrum. These facts suggest that the meteor was produced by a silicate rich stony meteoroid.

The spectrum shows two minor changes along the trajectory. They can be seen in Fig. 11. Firstly, the low-excitation inter-combination lines, in particular Fe I multiplet 2, are enhanced at 0.50 s, at the brightest point of the meteor. Inter-combination lines are commonly seen to be bright in meteor spectra, especially in the meteor wake. O 27471 does not show significant wake and those lines probably originate in the outer parts of the radiating region which are not in thermal equilibrium.

The second change is the increasing strength of calcium lines relatively to other lines toward lower heights. Calcium is underabundant in the radiating gas due to incomplete evaporation but the evaporation efficiency increases at lower heights. Also this effect is common in meteors of similar velocity (Borovička 1993; Ceplecha et al. 1998).

In summary, in this spectrum we did not find any evidences which could explain the changes of the shape-density coefficient K. The changes of K are not represented in the radiation of the meteor, at least in the visual range and above our sensitivity limit.

7.3. Large values of K at the start of luminous trajectories

The large K at the start of almost all examined cases with precise observational data calls for explanation. There are several possibilities.

1. All the effect is from changing bulk density (outer layers composed of low density material.
2. Changing head cross-section e.g. due to rotation.
3. The air density is widely and systematically different from the used model (CIRA 72)
4. Eq. (1) is not valid and needs some large additional term at the trajectory start

Explanation 1 should be recognizable in spectral records. Even if we are not definitive with our limited spectral analysis, we feel this explanation of so large values of K very improbable. Explanation 2 may be well right, but some of the K values are so large that only an extremely flat shape could explain them, and we are not much inclined to assume that these cases correspond to meteoroids thin as a sheet of paper. Something which is in favor of explanation 2: periodic changes of decelerations and of K at the early parts of the trajectories may well represent rotation of the body. We found periods between 2 and 4 rotations per second for different events. Explanation 3 seems very improbable. One needs changes of the air density against the CIRA 72 model by a factor of the order of 10 on a height differences of the order of 10 km. All these explanations 1 to 3 may act together. But if we take into account that large values of K are typical explanation of almost all differences from the assumption of constant K and σ, and if we draw our attention to anomalous cases with positive values of $\frac{\mathrm{d}v}{\mathrm{d}t}$ during an extensive part of the trajectory (e.g. Fig. 10), we are inclined to accept explanation 4 as the most probable.

Revision of the basic differential equations is not in the scope of this paper, but we feel that some hints on what is omitted in Eq. (1) are necessary. It should be a rather large additional term, having occasionally about the same value as the existing term at the beginning of trajectories. Omitted gravity term is insignificant in this sense for all examined cases. In this respect some authors in the past mentioned reverse rocket effect (Levin 1961; Bronshten 1983). However, there is another possibility: a meteoroid penetrating through the ionospheric layers is electrically charged (in addition to its original interplanetary charge) and then interferes with much larger volumes of the atmosphere than it would be in case of only aerodynamic drag, and interferes also with the atmospheric electrical charges alternatively decelerating or accelerating the meteoric body.

This problem adds more uncertainty to results on individual meteoroids. Many times in the past we mentioned that meteoroids in the atmosphere behave very individually. It has no sense to speak about an average meteoroid (inclusive meteor showers). Now we are adding another “individualism”, the state

of the ionospheric layers and electric charge of the meteoroid, which could change atmospheric meteoroid trajectory so much like do the differences among them. In any case we want to devote more attention to this problem in some of our future studies. Very precise trajectories observed, immediate state of the entire atmosphere from all aspects, and good luck for anomalous events to be recorded, this is all we need to proceed to some more general insight into problems of meteoroid interaction with the atmosphere.

Acknowledgements. Our sincere thanks are due to Ing. J. Keclíková for her work with measuring original photographic records. We are very much obliged to Dr. R.E. McCrosky for lending us films from his PN archive. We very much appreciated discussions with Dr. R.E. Spalding, which led us to suspect electric properties of the atmosphere and of the meteor phenomenon are important for making the decelerations so anomalous and not explainable in scope of only mechanical and thermodynamical forces. We are pleased to announce that this work has been supported by Contract AJ–4706 of the Sandia National Laboratories, and by the Grant Agency of the Czech Republic (205/97/0700).

References

Borovička J., 1993, A&A 279, 627
Bronshten V.A., 1983, Physics of Meteor Phenomena. D.Reidel Publ. Co., Dordrecht, Holland, p. 356
Ceplecha Z., Padevět V., 1969, Bull. Astr. Inst. Czech. 20, 117
Ceplecha Z., McCrosky R.E., 1997, Meteorit. Planetary Sci. 32, A157
Ceplecha Z., Spurný P., Borovička J., et al., 1993, A&A 279, 615
Ceplecha Z., Borovička J., Elford W.G., et al., 1998, Space Sci. Rev. 84, 327
Ceplecha Z., Spurný P., Borovička J., 2000, http://www.asu.cas.cz/∼ceplecha/precbol.html
CIRA 72, 1972, COSPAR International Reference Atmosphere 1972, Akademie Verlag, Berlin
Levin (Lewin) B.J., 1961, Theorie der Meteore und die meteorische Substanz im Sonnensystem. Scientia Astronomica 4, Akademie Verlag, Berlin, p. 330
McCrosky R.E., Shao C.-Y., Posen A., 1976, Prairie network fireball data I: summary and orbits. Center Astrophys. Prepr. Ser. 665
McCrosky R.E., Shao C.-Y., Posen A., 1977, Prairie network fireball data II: trajectories and light curves. Center Astrophys. Prepr. Ser. 721
Pecina P., Ceplecha Z., 1983, Bull. Astron. Inst. Czechosl. 34, 102
Pecina P., Ceplecha Z., 1984, Bull. Astron. Inst. Czechosl. 35, 120
Spurný P., 1997, Proc. SPIE 3116, 144